CHEMISTRY OF MATERIALS

Article

pubs.acs.org/cm

pH Responsive and Oxidation Resistant Wet Adhesive based on Reversible Catechol−Boronate Complexation

Ameya R. Narkar, Brett Barker, Matthew Clisch, Jingfeng Jiang, and Bruce P. Lee*

Department of Biomedical Engineering, Michigan Technological University, 1400 Townsend Drive, Houghton, Michigan 49931, United States

Supporting Information

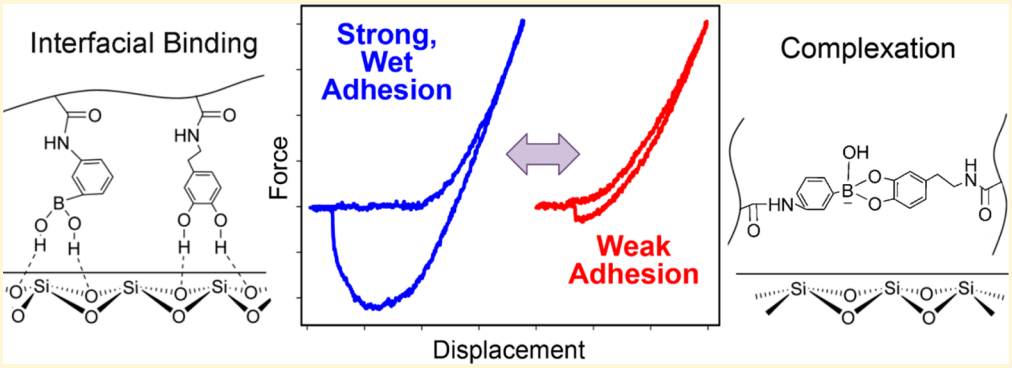

ABSTRACT: A smart adhesive capable of binding to a wetted surface was prepared by copolymerizing dopamine methacrylamide (DMA) and 3-acrylamido phenylboronic acid (AAPBA). pH was used to control the oxidation state and the adhesive property of the catechol side chain of DMA and to trigger the catechol−boronate complexation. FTIR spectroscopy confirmed the formation of the complex at pH 9, which was not present at pH 3. The formation of the catechol−boronate complex increased the cross-linking density of the adhesive network. Most notably, the loss modulus values of the adhesive were more than an order of magnitude higher for adhesive incubated at pH 9 when compared to those measured at pH 3. This drastic increase in the viscous dissipation property is attributed to the introduction of reversible complexation into the adhesive network. Based on the Johnson Kendall Roberts (JKR) contact mechanics test, adhesive containing both DMA and AAPBA demonstrated strong interfacial binding properties (work of adhesion (W_{adh}) = 2000 mJ/m^2) to borosilicate glass wetted with an acidic solution (pH 3). When the pH was increased to 9, W_{adh} values (180 mJ/m^2) decreased by more than an order of magnitude. During successive contact cycles, the adhesive demonstrated the capability to transition reversibly between its adhesive and nonadhesive states with changing pH. Adhesive containing only DMA responded slowly to repeated changes in pH and became progressively oxidized without the protection of boronic acid. Although adhesive containing only AAPBA also demonstrated strong wet adhesion (W_{adh} ∼ 500 mJ/m^2), its adhesive properties were not pH responsive. Both DMA and AAPBA are required to fabricate a smart adhesive with tunable and reversible adhesive properties.

INTRODUCTION

A smart adhesive can switch between its adhesive and nonadhesive states in response to externally applied stimuli. The ability to control interfacial binding properties on command is of critical interest in various fields of materials science and engineering, including manufacturing, development of sustainable packaging, repair of complex structural components, and development of painlessly removable wound dressings.[1−4] However, existing smart adhesives are limited by the need for extreme conditions to promote debonding (e.g., elevated temperature),[2] adhesion to only a specific type of substrate,[5] or weakened adhesive strength under moist conditions.[3] Smart adhesives reported to-date have demonstrated adhesion predominately to dry surfaces. The performance of most man-made adhesives is significantly compromised in the presence of moisture, as water effectively competes for surface bonding and eliminates contributions of van der Waals' interaction.[6,7]

Marine mussels secrete adhesive proteins that enable them to bind to various surfaces (rocks, piers, etc.) in a saline and wet environment.[8,9] One of the main structural components in these adhesive proteins is the presence of a unique catechol-based amino acid, L-3,4-dihydroxyphenylalanine (DOPA), which is responsible for interfacial binding and rapid solidification of the proteins.[7] Modification of inert polymers with catechol groups imparted these materials with strong adhesive properties to both organic and inorganic substrates.[10−12] Additionally, the unique and versatile phenolic chemistries

Received: May 9, 2016
Revised: July 12, 2016
Published: July 14, 2016

DOI: 10.1021/acs.chemmater.6b01851
Chem. Mater. 2016, 28, 5432−5439

have enabled scientists to design stimuli responsive films,[13] self-healing networks,[14] shape-changing actuators,[15−17] and self-assembled capsules.[18] Although smart adhesives inspired by mussel adhesive chemistry have been recently reported, these adhesives demonstrated limited reversibility (i.e., one time activation[19] or one time deactivation[20]).

The adhesive strength of catechol is highly dependent on its oxidation state (Scheme 1).[21−23] The interaction between the reduced form of catechol and titanium (Ti) surface was reported to average around 800 pN, which is 40% that of a covalent bond.[24] When the catechol was oxidized to its quinone form in a basic pH (Scheme 1b), a drastic reduction in the pull-off force (180 pN) was observed.[24] This indicates that the oxidation state of catechol can be used to tune the adhesive property of this biomimetic adhesive moiety. However, the quinone is highly reactive and can participate in irreversible covalent cross-linking (Scheme 1c),[25,26] which will potentially limit the catechol's ability to function as a reversible adhesive moiety.

Scheme 1. Reduced Form of Catechol Is Responsible for Strong Interfacial Binding (a), while the Oxidized Quinone Exhibits Weak Adhesion (b); Quinone Is Also Highly Reactive and Can Undergo Irreversible Covalent Crosslinking (c)

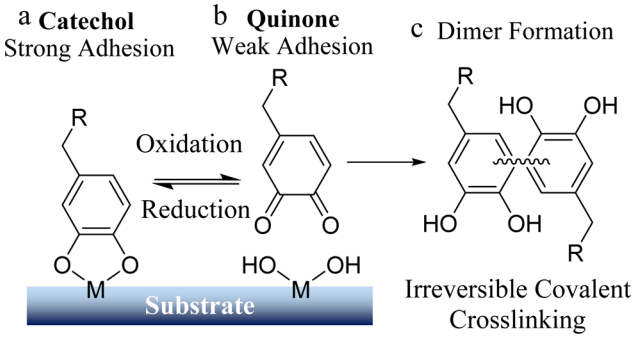

To preserve the reversibility of catechol, the smart adhesive reported here is composed of network-bound phenylboronic acid. Catechol forms a pH-dependent, reversible complex with boronic acid.[27] This complex is strong enough to form a self-healing polymer network with modulus approaching those of covalently cross-linked networks.[28] Boronic acid has also been previously used as a temporary protecting group for the synthesis of DOPA-modified polymers, while preserving the reactivity of its catechol side chain.[29] Additionally, the presence of boronic acid has been demonstrated to reduce the adhesive strength of a catechol-based adhesive.[30] Recently, this coordination chemistry was used to design pH responsive capsules for drug delivery.[31]

We hypothesize that the incorporation of the network-bound boronic acid can provide a protecting mechanism for catechol against irreversible oxidation cross-linking and to preserve the reversibility of the interfacial binding properties of catechol-containing smart adhesive. To this end, adhesive hydrogels were prepared by the copolymerization of dopamine methacrylamide (DMA) and 3-acrylamido phenylboronic acid (AAPBA). DMA contains a catechol side chain that mimics the adhesive properties of DOPA. The formation of the catechol−boronate complex in the adhesive network was characterized by infrared spectroscopy, equilibrium swelling, and oscillatory rheometry experiments. The effect of the complex on the reversibility of adhesive properties was characterized using Johnson Kendall Roberts (JKR) contact mechanics test.

MATERIALS AND METHODS

Materials. *N*-Hydroxyethyl acrylamide (HEAA) and AAPBA were purchased from Sigma-Aldrich. 2,2-Dimethoxy-2-phenylacetophenone (DMPA) and methylene bis-acrylamide (MBAA) were purchased from Acros Organics. Dimethyl sulfoxide (DMSO) was purchased from Macron. Ethanol (190 proof) was purchased from Pharmco Aaper. DMA was synthesized following published protocols.[32] The acidic solution was prepared by titrating a 0.1 M NaCl solution to pH 3 using 1 M HCl, while the basic buffer medium was prepared by titrating 10 mM Tris (hydroxymethyl)aminomethane (Tris) base with 1 M HCl to pH 9.

Preparation of the Adhesive Hydrogel. Adhesive hydrogels were prepared by curing a precursor solution containing 1 M of HEAA with up to 10 mol % each of DMA and AAPBA dissolved in 40% (v/v) DMSO in deionized (DI) water. The bifunctional cross-linker (MBAA) and the photoinitiator (DMPA) were kept at 3 and 0.1 mol %, respectively, relative to HEAA. The precursor solutions were degassed three times, added to a mold with a spacer (2 mm thick), and photoinitiated in a UV cross-linking chamber (XL-1000, Spectronics Corporation, Westbury, NY) located in a nitrogen-filled glovebox (PLAS LABORATORIES, Lansing, MI) for 600 s.[15,16] To form a hemispherical gel, 50 μL of solutions were pipetted on to a fluorinated glass slide (refer to protocol in the Supporting Information) and photoinitiated for 600 s. Depending on the experiment, the hydrogels were equilibrated in either the acidic (pH 3) or basic (pH 9) solutions for 24−48 h with gentle nutation and frequent medium changes prior to subsequent experimentation. The adhesive compositions are abbreviated as D*x*B*y* where the *x* and *y* stand for the mol % of DMA and AAPBA, respectively, relative to the concentration of HEAA.

Equilibrium Swelling. Hydrogel discs (thickness = 2 mm and diameter = 15 mm) were rinsed briefly (for about 10 s) in DI water and equilibrated in 5 mL of either the acidic solution (pH 3) or basic (pH 9) buffer medium for 48 h, with continuous and gentle nutation. The samples were dried under vacuum for at least 48 h. Both the swollen (M_s) and dry (M_d) masses of the samples were used to determine the equilibrium swelling ratio using the following equation:[33]

$$\text{Equilibrium Swelling} = \frac{M_s}{M_d} \quad (1)$$

Fourier Transform Infrared (FTIR) Spectroscopy. The samples were freeze-dried, crushed into fine powder using a mortar and pestle, and analyzed using a PerkinElmer Frontier Spectrometer fitted with a GladiATR accessory from Pike Technologies.

Oscillatory Rheometry. Hydrogel samples (15 mm diameter and 2 mm thick) were equilibrated in pH 3 or 9 with nutation for 48 h and compressed to a constant gap of 1800 μm using a 20 mm diameter parallel plate geometry. The storage (G') and loss (G'') moduli were determined in the frequency range of 0.1−100 Hz and at a strain of 8% using a TA Discovery Hybrid Rheometer-2 (TA Instruments).

Contact Mechanics Test. Contact mechanics tests were performed using the JKR indentation method to determine the interfacial binding properties of the hydrogels. A custom-built indentation device comprising a 10-g load cell (Transducer Techniques), high resolution miniature linear stage stepper motor (MFA-PPD, Newport), and an indenter (ALS-06, Transducer Techniques) for affixing a hemispherical gel was used to conduct the contact mechanics testing (Scheme 2).[34]

Two contact mechanics tests were performed. In the first test, samples were equilibrated at pH 3 or 9 for 48 h prior to testing to determine the effect of pH on their adhesive properties. The hemispherical gel was affixed to the indenter using Super Glue (Loctite Professional Liquid) and was compressed at 1 μm/s until reaching a maximum preload of 20 mN. The gel sample was retracted at the same rate. A borosilicate glass surface (Pearl microscope slides,

DOI: 10.1021/acs.chemmater.6b01851
Chem. Mater. 2016, 28, 5432−5439

Scheme 2. Schematic Representation of the Setup Used in the Contact Mechanics Adhesion Testing

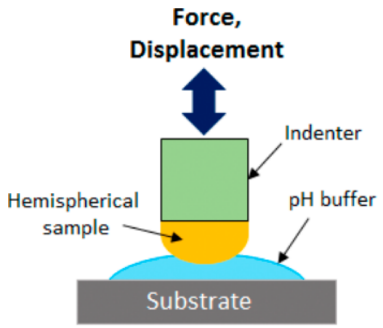

cat. no. 7101) was used as test substrate, and it was wetted with 25 μL of either pH 3 solution or pH 9 buffer medium.

In the second test, the reversibility of the adhesive to transition between its adhesive and nonadhesive states in response to pH change was examined. The samples were first equilibrated in the pH 3 solution for 24 h with gentle nutation before testing. Reversible adhesion testing was conducted on both a borosilicate glass surface and a quartz surface (Tedpella, Inc., product no. 26011, Redding, CA). A single hydrogel sample was subjected to three successive contact cycles on the substrate surface wetted with 25 μL of solution maintained at different pH levels (i.e., pH 3, 9, and then 3 for cycles 1, 2, and 3, respectively). In between cycles, the hemispherical gels were briefly incubated in 100 μL of solution (i.e., pH 9 and 3, after cycles 1 and 2, respectively) for 10 min. After removing 75 μL of the solution, the test was carried out in the presence of the remaining 25 μL of the solution.

The force (F) versus displacement (δ) curves were integrated to determine the work of adhesion (W_{adh}), which was normalized by the maximum area of contact (A_{max}) using the following equation:[35]

$$W_{adh} = \frac{\int F \, d\delta}{A_{max}} \tag{2}$$

To mathematically calculate A_{max}, the loading portion of the contact curve was fitted with the Hertzian model:[36]

$$\delta_{max} = \frac{a^2}{R} \tag{3}$$

where δ_{max} is the maximum displacement at the maximum preload of 20 mN, a is the radius of A_{max}, and R is the radius of curvature of the hemispherical gel. The height (h) and base radius (r) of each individual hemisphere were measured using a digital vernier caliper before testing to determine R:[37]

$$R = \frac{h}{2} + \frac{r^2}{2h} \tag{4}$$

A_{max} was determined using the following equation:

$$A_{max} = \pi a^2 \tag{5}$$

Finally, the maximum adhesive force (F_{max}) was determined as the highest negative load recorded in the force vs displacement curve.

Statistical Analysis. Statistical analysis was carried out using JMP Pro 12 software (SAS Institute, NC). Student's t test and one way analysis of variance (ANOVA) with Tukey–Kramer HSD analysis were performed for comparing means between two and multiple groups, respectively. $p < 0.05$ was considered significant.

RESULTS AND DISCUSSION

Hydrogels were prepared with a neutral monomer (HEAA) and network-bound catechol (DMA) and phenylboronic acid (AAPBA) side chains. We utilize pH to control the oxidation state of the catechol group and its interfacial binding strength. pH 3 was chosen in order to examine the adhesive properties of the reduced from of catechol (i.e., adhesive state).[23,30] Conversely, pH 9 was chosen to examine the adhesive properties of the oxidized form of the catechol (i.e., nonadhesive state) with weakened interfacial binding strength[23,38] and to induce the formation of the catechol–boronate complex. The ideal pH (pH_{ideal}) for effective interaction between a diol and a boronic acid has been reported to be the average of their respective acid dissociation constant (pK_a) values ($pH_{ideal} = (pK_{aacid} + pK_{adiol})/2$).[39] Given the reported pK_a values for catechol ($pK_{adiol} = 9.3$)[40] and phenylboronic acid ($pK_{aacid} = 8.8$),[40,41] pH 9 ($(9.3 + 8.8)/2 \approx 9$) is an ideal pH for promoting complexation between DMA and AAPBA.

Qualitative Analysis. Photographs of hydrogels incubated in pH 3 or 9 for 48 h confirmed that pH effectively controlled the oxidation states of DMA (Table S1). Both D10B0 and D10B10 remained colorless after incubation in pH 3, indicating that the acidic pH preserved the reduced state of the catechol. However, D10B0 developed a dark brown color (tanning of catechol) when it was incubated in pH 9, which is indicative of the oxidation of catecholic groups to quinone.[26,42] On the other hand, D10B10 developed a slight pinkish tinge at pH 9, indicating that the introduction of boronic acid groups protected the catechol from undergoing oxidation. Samples that were catechol-free (e.g., D0B0 and D0B10) did not display any coloration at both pH levels.

Equilibrium Swelling. Hydrogels were equilibrated at either pH 3 or 9 to determine the effect of pH on their swelling ratio (Figure 1). D0B0 did not exhibit any significant change in its swelling ratio with changing pH, confirming that the poly(HEAA) backbone is not pH responsive. Increasing the DMA content to 10 mol % (e.g., D10B0) decreased the swelling ratio of the hydrogel as a result of increased hydrophobicity with the incorporation of the benzene ring in DMA. This change in swelling may also be attributed to the increased molecular interactions between the benzene rings (i.e., π–π interactions, hydrogen bonding). At pH 9, D10B0 exhibited an increase in swelling ratio when compared to pH 3 (30% increase), potentially due to the increased formation of negatively charged semiquinone with increasing pH (Scheme S1A).[43] Similarly, D0B10 exhibited a higher swelling ratio at pH 9. Phenylboronic acid transforms into a negatively charged trigonal structure when the pH value approaches and becomes higher than its pK_a value ($pK_a = 8.8$, Scheme S1B).[39] Similar

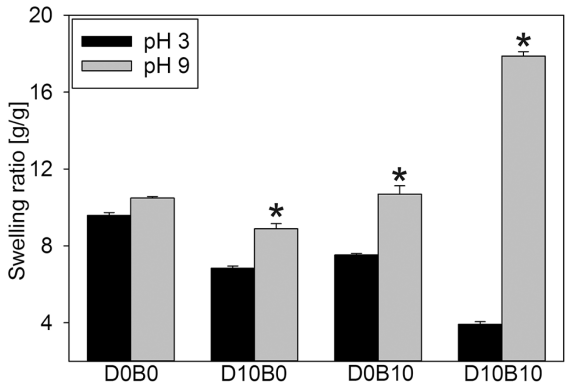

Figure 1. Swelling ratio of adhesives equilibrated at either pH 3 or 9 ($n = 3$). *$p < 0.05$ when compared to the adhesive equilibrated at pH 3 for a given composition.

DOI: 10.1021/acs.chemmater.6b01851
Chem. Mater. 2016, 28, 5432–5439

pH dependent swelling has been previously reported for phenylboronic acid containing hydrogels.[44]

Hydrogels containing both DMA and AAPBA exhibited maximum shrinkage in the acidic solution and maximum swelling in the basic medium. A drastic reduction in swelling at the acidic pH is likely due to the hydrophobicity of the benzyl ring in both DMA and AAPBA as well as their ability to form physical bonds. At pH 9, formation of the catechol−boronate complex results in the formation of negative charge and extensive swelling as a result of electrostatic repulsion (Scheme S1C).[39,44] This pH dependent swelling was observed for hydrogel formulations that contained various amounts of DMA and AAPBA (Figure S1). D10B10 contained the highest mol % of both DMA and AAPBA and exhibited the largest difference in the swelling ratio between pH 3 and 9 (an increase of 360%).

FTIR. FTIR spectra confirmed the characteristics peaks for HEAA (−OH 3400−3000 cm^{-1}, secondary amide−NH 1680−1630 cm^{-1}, and C═O 1600−1500 cm^{-1}) and benzene rings (1500−1400 and 800−700 cm^{-1}) in D10B10 (Figure 2).[45,46]

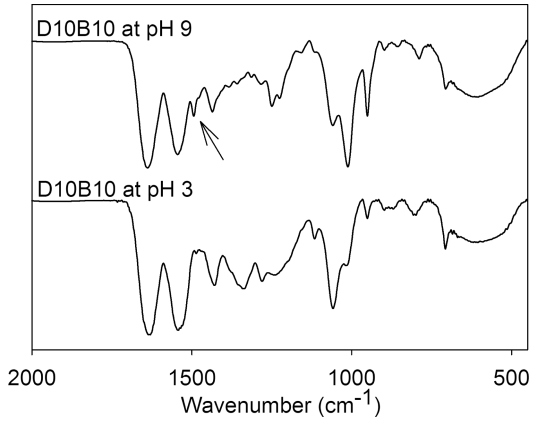

Figure 2. FTIR spectra of D10B10 equilibrated at either pH 3 or 9. The arrow points to the presence of a new peak (1489 cm^{-1}) found at pH 9, corresponding to the formation of catechol−boronate complex.

When comparing spectra of D10B10 incubated at different pH levels, a new peak was observed at 1489 cm^{-1} at pH 9 (arrow in Figure 2), which was not present when D10B10 was incubated at pH 3. This new peak is associated with the benzene ring stretch in aromatic compounds as a result of changing their vibrational states. This peak compares favorably with values (1478−1501 cm^{-1}) previously reported for the catechol−boronate complex.[47] This peak was not present in samples that did not contain both DMA and AAPBA (i.e., D0B0, D10B0, or D0B10) tested at both pH 3 and 9 (Figure S2).

Oscillatory Rheometry. Oscillatory rheometry results indicated that regardless of composition, all the hydrogels were chemically cross-linked, as the G' values were independent of frequencies (<45 Hz) and the G' values were 1−2 orders of magnitude higher than the G'' values (Figure 3 and Figure S3). There were minimal differences in both the G' and G'' values for the various control groups (D0B0, D10B0, and D0B10) equilibrated at different pH levels (Figure S3). On the other hand, D10B10 exhibited an increase in the G' value (a 55% increase at a frequency of 1 Hz) when the pH was increased from pH 3 to 9 (Figure 3). An increase in the measured stiffness is a result of increasing cross-linking density, resulting from the formation of new intermolecular cross-links within the hydrogel network.

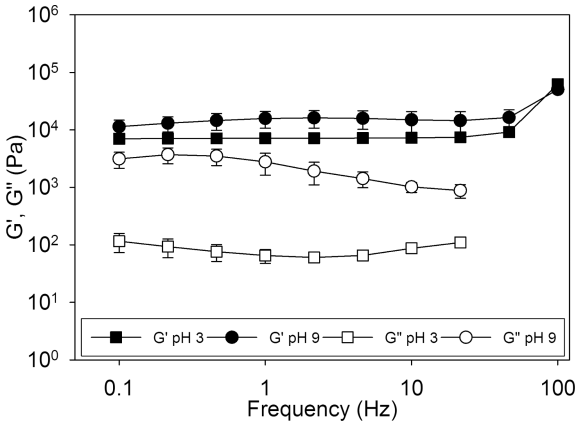

Figure 3. Storage (G', filled symbol) and loss (G'', open symbol) moduli for D10B10 equilibrated at either pH 3 (■, □) or 9 (●, ○) (n = 3).

Most notably, D10B10 incubated at pH 9 exhibited G'' values that were an order of magnitude higher than those incubated at pH 3. This increase in viscous dissipation properties indicates the presence of extensive reversible physical interaction in the hydrogel network attributed to catechol−boronate complexation at pH 9.[48,49] These enhancements in mechanical properties are remarkable considering these complexes needed to counteract the extensive swelling of the network resulting from electrostatic repulsion of the negatively charged complexes (Scheme S1C). This may explain why there was only a marginal increase in the measured G' values in response to changes in pH. Similar pH dependent behaviors were observed for hydrogels containing various ratios of DMA and AAPBA (Figure S4).

Contact Mechanics Testing of Equilibrated Adhesive. JKR contact mechanics tests were performed to determine the effect of pH on the interfacial binding properties of the adhesive. D0B0 exhibited minimal interaction with the substrate at both pH levels as expected (Figure S5a, Table 1). Incorporation of 10 mol % DMA (D10B0) significantly increased the measured adhesive properties at pH 3 (Figure S5b). This indicates that the reduced form of catechol is responsible for strong interfacial binding, potentially through H-bonding or electrostatic interaction with silicon dioxide (SiO_2), which is a major component of borosilicate glass.[50] Density functional theory analysis revealed that catechol readily displaces water molecules to bind to SiO_2 surface, with a binding energy (33 kcal/mol) value approaching that of catechol−Ti interaction.[51,52] D10B0 incubated at pH 9 exhibited a significant reduction in adhesive properties. Specifically, the measured W_{adh} value for D10B0 measured at pH 9 was not significantly different from that of D0B0.

Interestingly, D0B10 also demonstrated equivalent or higher adhesive properties when compared to its counterparts (Figure S5c). Although the interaction between boronic acid and glass substrates has not been previously reported, AAPBA likely interacted with the surface via H-bonding or electrostatic interaction. However, D0B10 also exhibited significantly higher F_{max} values at pH 9 when compared to D10B0 and D0B0. This indicates that the incorporation of AAPBA alone was not sufficient in creating a smart adhesive due to its ineffective pH responsive characteristics.

At pH 3, D10B10 demonstrated significantly higher F_{max} (−11 ± 1.6 mN) and W_{adh} (460 ± 110 mJ/m^2) values relative

DOI: 10.1021/acs.chemmater.6b01851
Chem. Mater. 2016, 28, 5432−5439

Table 1. Average F_{max} and W_{adh} Values Calculated for Adhesives Containing Varying Amounts of DMA and AAPBA Equilibrated and Tested at Either pH 3 or 9 (n = 3)

	F_{max} (mN)		W_{adh} (mJ/m^2)	
composition	pH 3	pH 9	pH 3	pH 9
D0B0	−1.4 ± 0.25	−0.85 ± 0.24	100 ± 24	76 ± 11
D10B0	−5.9 ± 0.45	−1.6 ± 0.67	170 ± 12	83 ± 28
D0B10	−6.6 ± 0.46	−4.1 ± 0.38	240 ± 28	96 ± 19
D10B10	−11 ± 1.6	−1.1 ± 0.020	460 ± 110	110 ± 6.6

to those obtained from D10B0 and D0B10 (Figure 4, Table 1). This indicates that both DMA and AAPBA contributed to

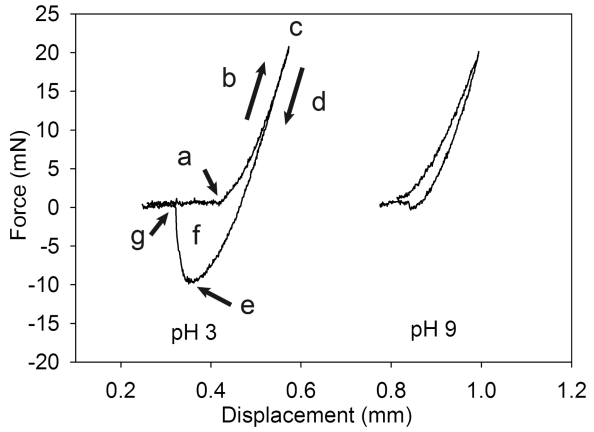

Figure 4. Representative contact curves for D10B10 equilibrated and tested at either pH 3 (left) or 9 (right). The lowercase letters indicate the point of initial contact with the borosilicate glass surface (a), the loading portion of the curve (b), the maximum preload (c), the unloading portion of the curve (d), the maximum adhesive force (F_{max}; e), the area enclosed by the curve corresponding to W_{adh} (f), and the point of detachment from the substrate (g).

surface adhesion. At the same time, D10B10 exhibited a 10 and 4.2 times reduction in F_{max} and W_{adh} values, respectively, at pH 9, indicating that the formation of catechol−boronate complex successfully reduced interfacial binding.

Reversibility Adhesion Testing. To confirm the reversible nature of the catechol−boronate complex and its contribution to interfacial binding, samples were repeatedly brought into contact with the substrate while exposing the adhesive to solutions with different pHs. D0B0 exhibited very low adhesive values for all three contact cycles (Figure S6). D10B0 demonstrated strong adhesion during the first contact cycle performed at pH 3 (Figure 5a). However, unlike values obtained from D10B0 that were equilibrated for 48 h (Figure S5b, Table 1), there was no significant change in the measured adhesive values in the second contact cycle measured at pH 9. This may be due to the adhesive's short exposure time to the basic medium and slow oxidation of the catechol to quinone. However, both F_{max} and W_{adh} values were significantly lower in the third contact cycle performed at pH 3. The adhesive network likely traps the basic medium during the second contact cycle, and the catechol groups became progressively oxidized with time. D0B10 did not exhibit changes in its adhesive properties with changes in pH (Figure 5b).

D10B10 demonstrated elevated adhesive properties (F_{max} = −16 ± 0.60 mN, W_{adh} = 2000 ± 250 mJ/m^2) during the first contact cycle at pH 3, with adhesion values that were 2−3 folds higher when compared to values obtained for D10B0 and

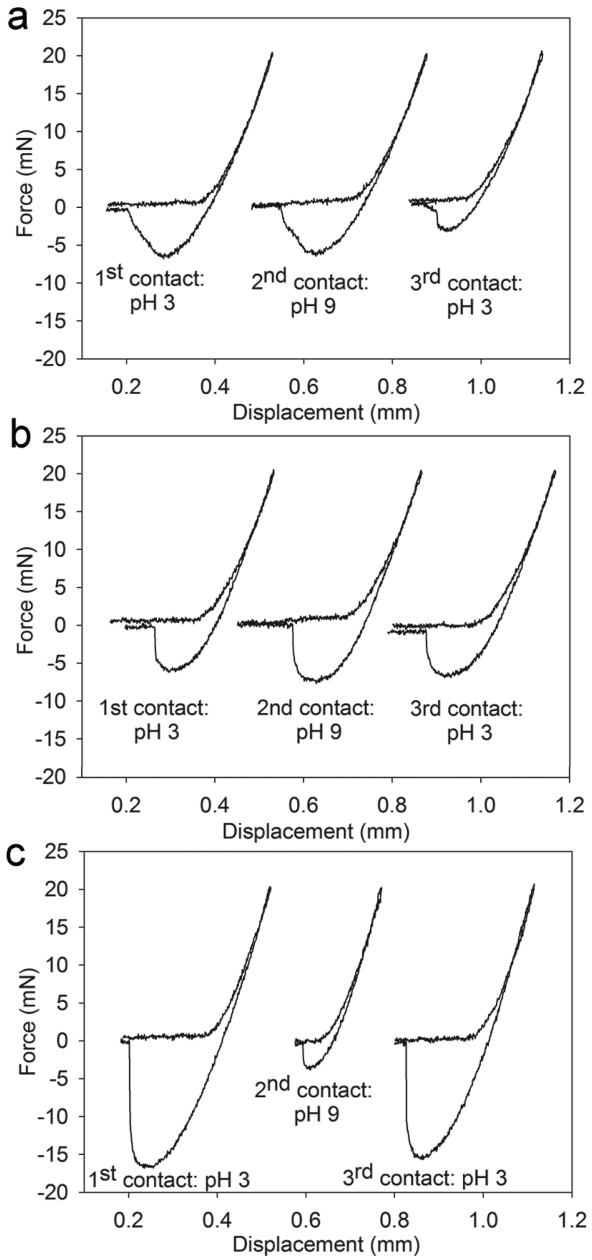

Figure 5. Three successive contact curves for D10B0 (a), D0B10 (b), and D10B10 (c) tested at pH 3, pH 9, and then pH 3 using a borosilicate glass substrate.

D0B10 (Figures 5 and 6). During the second contact at pH 9, these values were reduced by more than an order of magnitude (F_{max} = −2.4 ± 1.1 mN, W_{adh} = 180 ± 87 mJ/m^2). These values were two to three times lower when compared to those measured for D10B0 and D0B10, and they were also not

DOI: 10.1021/acs.chemmater.6b01851
Chem. Mater. 2016, 28, 5432−5439

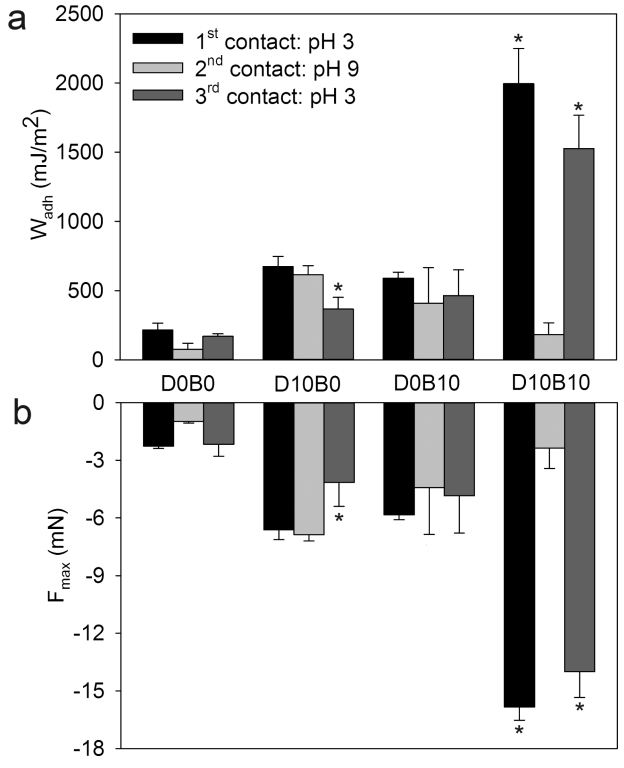

Figure 6. Averaged W_{adh} (a) and F_{max} (b) for adhesives tested in three successive contact cycles using a borosilicate glass as the substrate (n = 3). *p < 0.05 relative to the values obtained from the second contact cycle at pH 9 for a given formulation.

significantly different from those of D0B0. In the third contact cycle measured at pH 3, D10B10 recovered 90 and 76% of the F_{max} and W_{adh} values, respectively, measured during the first contact cycle.

Similar pH responsive trends were observed using the quartz surface (Figure S7). D10B10 demonstrated an order of magnitude difference between its adhesive (pH 3) and nonadhesive (pH 9) states. Similarly, D10B0 demonstrated reduced adhesion with successive contact cycles while D0B10 was not pH responsive. Lower adhesive values were obtained for quartz (~14% reduction for D10B10) when measured at pH 3 indicating that boron (~13%) in the borosilicate glass contributed to adhesion.

Taken together, adhesives containing DMA exhibited strong interfacial binding properties at pH 3, confirming previously published results that the reduced form of catechol is responsible for strong wet adhesion to inorganic substrates.[22,23,38] With extensive incubation time at pH 9, the catechol groups were oxidized and exhibited reduced adhesive properties. However, pH-mediated oxidation was relatively slow. The interfacial binding properties of DMA-containing adhesive did not respond to repeated changes in pH, but its adhesive properties decreased progressively with repeated contact. Phenylboronic acid also demonstrated strong adhesion to borosilicate surfaces in the presence of water. However, adhesive containing only AAPBA was not pH responsive. These results indicated that adhesives containing either DMA alone or AAPBA alone were not suitable in functioning as a smart adhesive.

When an adhesive contained both DMA and AAPBA, both the catechol and phenylboronic acid moieties contributed to strong interfacial binding at pH 3 (Scheme 3). Elevating the pH

Scheme 3. Schematic Representation of the Smart Adhesive Containing Catechol and Phenylboronic Acid Functional Groups[a]

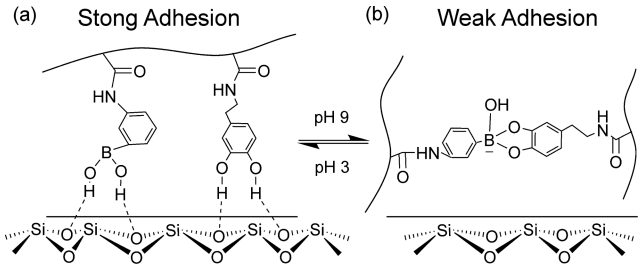

[a]At an acidic pH, both the catechol and borate functional groups contributed to strong interfacial binding with the wetted borosilicate substrate (a). In a basic pH, formation of catechol−boronate complexation reduced the interfacial binding strength of the adhesive (b). Changing the pH effectively converts the smart adhesive between its adhesive and non-adhesive states.

resulted in the formation of catechol−boronate complex and a significant reduction in the adhesive properties. The reversible nature of this complex allowed both the catechol and the phenylboronic acid moieties to become available for interfacial binding once the pH was reduced. AAPBA not only served as an adhesive moiety for interfacial binding, it also functioned as a protecting group to limit catechol oxidation. The combination of catechol and phenylboronic acid provides a basis for desiging a novel smart adhesive that is capable of switching between its adhesive and nonadhesive states in the presence of an aqueous environment. To our knowledge, this the first demonstration of a wet adhesive with tunable adhesive properties that exploits the chemistry found in mussel adhesive proteins.

CONCLUSIONS

Hydrogel adhesives containing DMA and AAPBA were prepared. FTIR, equilibrium swelling, and oscillatory rheometry experiments confirmed the formation of catechol−boronate complex at pH 9. JKR contact mechanics test revealed that adhesives containing both DMA and AAPBA exhibited elevated adhesive properties at pH 3, which were drastically reduced at pH 9. The reversible nature of the catechol−boronate complex enabled the adhesive to reversibly transition between its adhesive and nonadhesive states in response to pH change.

ASSOCIATED CONTENT

Supporting Information

The Supporting Information is available free of charge on the ACS Publications website at DOI: 10.1021/acs.chemmater.6b01851.

Protocol for preparing fluorinated glass slides, photographs of the adhesives, schematics of chemical structures, and additional results from swelling, FTIR, rheometry, and contact mechanics experiments (PDF)

AUTHOR INFORMATION

Corresponding Author

*Bruce P. Lee. E-mail: bplee@mtu.edu.

Funding

This project was supported by Office of Naval Research Young Investigator Award under Award Number N00014-16-1-2463 (B.P.L.) and National Institutes of Health under Award

DOI: 10.1021/acs.chemmater.6b01851
Chem. Mater. 2016, 28, 5432−5439

Numbers R15GM104846 (B.P.L.) and R15CA179409 (J.J.). A.R.N. was supported in part by the Kenneth Stevenson Biomedical Engineering Fellowship.

Notes

The authors declare no competing financial interest.

■ ACKNOWLEDGMENTS

The authors thank Randall Wilharm for the synthesis of DMA.

■ REFERENCES

(1) Heinzmann, C.; Coulibaly, S.; Roulin, A.; Fiore, G. L.; Weder, C. Light-Induced Bonding and Debonding with Supramolecular Adhesives. *ACS Appl. Mater. Interfaces* **2014**, *6* (7), 4713−4719.

(2) Northen, M. T.; Greiner, C.; Arzt, E.; Turner, K. L. A Gecko-Inspired Reversible Adhesive. *Adv. Mater.* **2008**, *20* (20), 3905−3909.

(3) Luo, X.; Lauber, K. E.; Mather, P. T. A thermally responsive, rigid, and reversible adhesive. *Polymer* **2010**, *51* (5), 1169−1175.

(4) Banea, M.; da Silva, L.; Campilho, R. An overview of the technologies for adhesive debonding on command. *Annals of "Dunarea de Jos" University of Galati. Fascicle XII: Welding Equipment and Technology* **2013**, *24*, 11−14.

(5) Sudre, G.; Olanier, L.; Tran, Y.; Hourdet, D.; Creton, C. Reversible adhesion between a hydrogel and a polymer brush. *Soft Matter* **2012**, *8* (31), 8184−8193.

(6) Comyn, J. The relationship between joint durability and water diffusion. In *Developments in Adhesives*; Kinloch, A. J., Ed.; Applied Science Publishers: Barking, U.K., 1981; Vol. 2, pp 279−313.

(7) Lee, B. P.; Messersmith, P. B.; Israelachvili, J. N.; Waite, J. H. Mussel-Inspired Adhesives and Coatings. *Annu. Rev. Mater. Res.* **2011**, *41*, 99−132.

(8) Waite, J. H. Nature's underwater adhesive specialist. *Int. J. Adhes. Adhes.* **1987**, *7* (1), 9−14.

(9) Yamamoto, H. Marine adhesive proteins and some biotechnological applications. *Biotechnol. Genet. Eng. Rev.* **1996**, *13*, 133−166.

(10) Meredith, H. J.; Wilker, J. J. The Interplay of Modulus, Strength, and Ductility in Adhesive Design Using Biomimetic Polymer Chemistry. *Adv. Funct. Mater.* **2015**, *25* (31), 5057−5065.

(11) Pechey, A.; Elwood, C. N.; Wignall, G. R.; Dalsin, J. L.; Lee, B. P.; Vanjecek, M.; Welch, I.; Ko, R.; Razvi, H.; Cadieux, P. A. Anti-adhesive coating and clearance of device associated uropathogenic escherichia coli cystitis. *J. Urol. (N. Y., NY, U. S.)* **2009**, *182* (4), 1628−1636.

(12) Liu, Y.; Meng, H.; Konst, S.; Sarmiento, R.; Rajachar, R.; Lee, B. P. Injectable Dopamine-Modified Poly(Ethylene Glycol) Nanocomposite Hydrogel with Enhanced Adhesive Property and Bioactivity. *ACS Appl. Mater. Interfaces* **2014**, *6* (19), 16982−16992.

(13) Ejima, H.; Richardson, J. J.; Liang, K.; Best, J. P.; van Koeverden, M. P.; Such, G. K.; Cui, J.; Caruso, F. One-step assembly of coordination complexes for versatile film and particle engineering. *Science* **2013**, *341* (6142), 154−157.

(14) Holten-Andersen, N.; Harrington, M. J.; Birkedal, H.; Lee, B. P.; Messersmith, P. B.; Lee, K. Y. C.; Waite, J. H. pH-induced mussel metal-ligand crosslinks yield self-healing polymer networks with near-covalent elastic moduli. *Proc. Natl. Acad. Sci. U. S. A.* **2011**, *108*, 2651−2655.

(15) Lee, B. P.; Konst, S. Novel hydrogel actuator inspired by reversible mussel adhesive protein chemistry. *Adv. Mater.* **2014**, *26* (21), 3415−3419.

(16) Lee, B. P.; Lin, M.-H.; Narkar, A.; Konst, S.; Wilharm, R. Modulating the Movement of Hydrogel Actuator based on Catechol-Iron Ion Coordination Chemistry. *Sens. Actuators, B* **2015**, *206*, 456−462.

(17) Lee, B. P.; Narkar, A.; Wilharm, R. Effect of metal ion type on the movement of hydrogel actuator based on catechol-metal ion coordination chemistry. *Sens. Actuators, B* **2016**, *227*, 248−254.

(18) Guo, J. L.; Ping, Y.; Ejima, H.; Alt, K.; Meissner, M.; Richardson, J. J.; Yan, Y.; Peter, K.; von Elverfeldt, D.; Hagemeyer, C. E.; Caruso, F. Engineering Multifunctional Capsules through the Assembly of Metal-Phenolic Networks. *Angew. Chem., Int. Ed.* **2014**, *53* (22), 5546−5551.

(19) Wilke, P.; Helfricht, N.; Mark, A.; Papastavrou, G.; Faivre, D.; Börner, H. G. A Direct Biocombinatorial Strategy toward Next Generation, Mussel-Glue Inspired Saltwater Adhesives. *J. Am. Chem. Soc.* **2014**, *136* (36), 12667−12674.

(20) Shafiq, Z.; Cui, J.; Pastor-Pérez, L.; San Miguel, V.; Gropeanu, R. A.; Serrano, C.; del Campo, A. Bioinspired Underwater Bonding and Debonding on Demand. *Angew. Chem., Int. Ed.* **2012**, *51* (18), 4332−4335.

(21) Yu, M.; Hwang, J.; Deming, T. J. Role of l-3,4-Dihydroxyphenylalanine in Mussel Adhesive Proteins. *J. Am. Chem. Soc.* **1999**, *121* (24), 5825−5826.

(22) Lee, B. P.; Chao, C.-Y.; Nunalee, F. N.; Motan, E.; Shull, K. R.; Messersmith, P. B. Rapid Gel Formation and Adhesion in Photocurable and Biodegradable Block Copolymers with High DOPA Content. *Macromolecules (Washington, DC, U. S.)* **2006**, *39* (5), 1740−1748.

(23) Yu, J.; Wei, W.; Menyo, M. S.; Masic, A.; Waite, J. H.; Israelachvili, J. N. Adhesion of Mussel Foot Protein-3 to TiO2 Surfaces: the Effect of pH. *Biomacromolecules* **2013**, *14* (4), 1072−1077.

(24) Lee, H.; Scherer, N. F.; Messersmith, P. B. Single-molecule mechanics of mussel adhesion. *Proc. Natl. Acad. Sci. U. S. A.* **2006**, *103* (35), 12999−13003.

(25) Yang, J.; Cohen Stuart, M. A.; Kamperman, M. Jack of all trades: versatile catechol crosslinking mechanisms. *Chem. Soc. Rev.* **2014**, *43* (24), 8271−8298.

(26) Lee, B. P.; Dalsin, J. L.; Messersmith, P. B. Synthesis and Gelation of DOPA-Modified Poly(ethylene glycol) Hydrogels. *Biomacromolecules* **2002**, *3* (5), 1038−1047.

(27) Pizer, R.; Babcock, L. Mechanism of Complexation of Boron Acids with Catechol and Substituted Catechols. *Inorg. Chem.* **1977**, *16* (7), 1677−1681.

(28) He, L.; Fullenkamp, D. E.; Rivera, J. G.; Messersmith, P. B. pH responsive self-healing hydrogels formed by boronate−catechol complexation. *Chem. Commun.* **2011**, *47*, 7497−7499.

(29) Huang, K.; Lee, B. P.; Ingram, D.; Messersmith, P. B. Synthesis and Characterization of Self-Assembling Block Copolymers Containing Bioadhesive End Groups. *Biomacromolecules* **2002**, *3* (2), 397−406.

(30) Kan, Y.; Danner, E. W.; Israelachvili, J. N.; Chen, Y.; Waite, J. H. Boronate Complex Formation with Dopa Containing Mussel Adhesive Protein Retards pH-Induced Oxidation and Enables Adhesion to Mica. *PLoS One* **2014**, *9* (10), e108869.

(31) Guo, J.; Sun, H.; Alt, K.; Tardy, B. L.; Richardson, J. J.; Suma, T.; Ejima, H.; Cui, J.; Hagemeyer, C. E.; Caruso, F. Boronate−Phenolic Network Capsules with Dual Response to Acidic pH and cis-Diols. *Adv. Healthcare Mater.* **2015**, *4* (12), 1796−1801.

(32) Lee, H.; Lee, B. P.; Messersmith, P. B. A reversible wet/dry adhesive inspired by mussels and geckos. *Nature (London, U. K.)* **2007**, *448* (7151), 338−341.

(33) Bryant, S. J.; Anseth, K. S. Hydrogel properties influence ECM production by chondrocytes photoencapsulated in poly(ethylene glycol) hydrogels. *J. Biomed. Mater. Res.* **2002**, *59* (1), 63−72.

(34) Yang, F. K.; Zhang, W.; Han, Y.; Yoffe, S.; Cho, Y.; Zhao, B. Contact" of Nanoscale Stiff Films. *Langmuir* **2012**, *28* (25), 9562−9572.

(35) Flanigan, C. M.; Crosby, A. J.; Shull, K. R. Structural development and adhesion of acrylic ABA triblock copolymer gels. *Macromolecules (Washington, DC, U. S.)* **1999**, *32* (21), 7251−7262.

(36) Hertz, H. On the contact of elastic solids. *J. Reine Angew. Math.* **1881**, *92*, 156−171.

(37) Shull, K. R.; Chen, W.-L. Fracture Mechanics Studies of Adhesion in Biological Systems. *Interface Sci.* **2000**, *8* (1), 95−110.

(38) Ding, X.; Vegesna, G. K.; Meng, H.; Winter, A.; Lee, B. P. Nitro-Group Functionalization of Dopamine and its Contribution to the Viscoelastic Properties of Catechol-Containing Nanocomposite Hydrogels. *Macromol. Chem. Phys.* **2015**, *216*, 1109−1119.

DOI: 10.1021/acs.chemmater.6b01851
Chem. Mater. 2016, 28, 5432−5439

(39) Yan, J.; Springsteen, G.; Deeter, S.; Wang, B. The relationship among pKa, pH, and binding constants in the interactions between boronic acids and diols—it is not as simple as it appears. *Tetrahedron* **2004**, *60* (49), 11205−11209.
(40) Springsteen, G.; Wang, B. A detailed examination of boronic acid−diol complexation. *Tetrahedron* **2002**, *58* (26), 5291−5300.
(41) Bull, S. D.; Davidson, M. G.; van den Elsen, J. M. H.; Fossey, J. S.; Jenkins, A. T. A.; Jiang, Y.-B.; Kubo, Y.; Marken, F.; Sakurai, K.; Zhao, J.; James, T. D. Exploiting the Reversible Covalent Bonding of Boronic Acids: Recognition, Sensing, and Assembly. *Acc. Chem. Res.* **2013**, *46* (2), 312−326.
(42) Meng, H.; Li, Y.; Faust, M.; Konst, S.; Lee, B. P. In *Hydrogen peroxide generation and biocompatibility of hydrogel-bound mussel adhesive moiety*; *Acta Biometerialia*, **2015**, *17*, 160−169.
(43) Kalyanaraman, B.; Felix, C. C.; Sealy, R. C. Semiquinone anion radicals of catechol(amine)s, catechol estrogens, and their metal ion complexes. *Environ. Health Perspect.* **1985**, *64*, 185−198.
(44) Kim, A.; Mujumdar, S.; Siegel, R. Swelling Properties of Hydrogels Containing Phenylboronic Acids. *Chemosensors* **2014**, *2* (1), 1−12.
(45) Sever, M. J.; Weisser, J. T.; Monahan, J.; Srinivasan, S.; Wilker, J. J. Metal-Mediated Cross-Linking in the Generation of a Marine-Mussel Adhesive. *Angew. Chem.* **2004**, *116* (4), 454−456.
(46) Lee, B. P.; Narkar, A.; Wilharm, R. Effect of metal ion type on the movement of hydrogel actuator based on catechol-metal ion coordination chemistry. *Sens. Actuators, B* **2016**, *227*, 248−254.
(47) Chen, G. C. Synthesis and evaluation of aminoborates derived from boric acid and diols for protecting wood against fungal and thermal degradation. *Wood Fiber Sci.* **2008**, *40* (2), 248−257.
(48) Skelton, S.; Bostwick, M.; O'Connor, K.; Konst, S.; Casey, S.; Lee, B. P. Biomimetic adhesive containing nanocomposite hydrogel with enhanced materials properties. *Soft Matter* **2013**, *9* (14), 3825−3833.
(49) Li, Y.; Meng, H.; Liu, Y.; Narkar, A.; Lee, B. P. Gelatin Microgel Incorporated Poly(ethylene glycol)-Based Bioadhesive with Enhanced Adhesive Property and Bioactivity. *ACS Appl. Mater. Interfaces* **2016**, *8* (19), 11980−11989.
(50) Chung, H.; Glass, P.; Pothen, J. M.; Sitti, M.; Washburn, N. R. Enhanced Adhesion of Dopamine Methacrylamide Elastomers via Viscoelasticity Tuning. *Biomacromolecules* **2011**, *12* (2), 342−347.
(51) Mian, S. A.; Gao, X.; Nagase, S.; Jang, J. Adsorption of catechol on a wet silica surface: density functional theory study. *Theor. Chem. Acc.* **2011**, *130*, 333−339.
(52) Mian, S. A.; Saha, L. C.; Jang, J.; Wang, L.; Gao, X.; Nagase, S. Density Functional Theory Study of Catechol Adhesion on Silica Surfaces. *J. Phys. Chem. C* **2010**, *114*, 20793−20800.

DOI: 10.1021/acs.chemmater.6b01851
Chem. Mater. 2016, 28, 5432−5439